Supplementary Material

Unless otherwise noted, reagents were obtained from Sigma-Aldrich (St. Louis, MO).

Cell Isolation and Construct Culture

Primary chondrocytes were isolated from articular cartilage of bovine calf (2 months old) carpometacarpal joints digested with type IV collagenase (activity = 747 U/g) in high glucose Dulbecco's Modified Eagle's Medium (hgDMEM) (Invitrogen, Carlsbad, CA) supplemented with 5% fetal bovine serum (Invitrogen), amino acids, buffering agents, and 1% antibiotic-antimycotic (Invitrogen) at 37 °C on a shaker for 6 hours (Lima et al., 2007). Cells were encapsulated in 2% agarose (type VII-A) at a density of 30×10^6 cells/mL. Constructs were cored from the cell-agarose mixture (∅4 mm × 2.3 mm thick) and cultured under static conditions for 45 days in chemically-defined, chondrogenic media (hgDMEM, 100 nM dexamethasone, 100 μg/mL sodium pyruvate, 50 μg/mL L-proline, 1% ITS+ premix (Becton Dickinson, Sparks, MD), 1% antibiotic-antimycotic, and 173 nmol/mL ascorbic acid 2-phosphate) at 37 °C under 5% CO_2 tension (Lima et al., 2007). Media were supplemented with 10 ng/mL TGF-β3 (R&D Systems, Minneapolis, MN) for either the entire culture period (β3+ group) or for only the first 14 days of culture (β3− group). A control group was cultured without TGF-β3 supplementation. Media were changed three times per week and conditioned media aliquots were taken at each media change.

Mechanical Characterization

Constructs (n = 4 per group and time point) were removed after 14, 28, and 45 days of culture. At each time point, constructs were mechanically tested in a custom device using unconfined compression with impermeable metal loading platens. Sample thickness and diameter were measured prior to loading. Samples were equilibrated under a creep load in a bath of phosphate buffered saline for 400 s. A stress relaxation test was then performed by ramping the displacement at a constant rate to 10% of the original thickness over 300 s, then relaxing for 1500 s. The stress relaxation data was curve-fitted to extract

mechanical properties similar to previous work (Cigan et al., 2013; Huang et al., 2012). This optimization analysis, performed in FEBio (febio.org), models the CTE constructs as a biphasic material consisting of both an intrinsically incompressible fluid and porous, solid matrix. Here, the solid matrix was modeled as a mixture of a neo-Hookean ground material (e.g., representing the scaffold material and GAG) and a continuous fiber distribution material (representing collagen) where fibers sustain tension only, with a linear variation of stress with strain (Ateshian et al., 2009). These fits were able to extract the equilibrium compressive modulus E_Y, the hydraulic permeability k, and the fiber modulus ξ. The optimization results fit the experimental data with $R^2 = 0.95 \pm 0.05$ (for all samples), a result consistent with prior results with similar engineered tissue constructs (Cigan et al., 2013; Huang et al., 2012).

Since fiber recruitment in a continuous fiber distribution model depends on the state of strain, the parameter ξ does not represent the actual tensile modulus of the construct. Therefore, the construct tensile modulus, E_T, was determined by modeling the equilibrium response to a homogeneous tensile deformation of a material with the same E_Y and ξ determined from the curve-fitting of the unconfined stress-relaxation response. In a prior study (Huang et al., 2012), it was shown that this method for predicting E_T from unconfined compression stress-relaxation experiments produced a value statistically not different from tensile test measurements.

Biochemical Analysis

After mechanical testing, constructs were radially halved and both halves were weighed. The construct masses were used to normalize the biochemical content and to calculate the swelling ratio for each group where normalized disk volume = (average construct mass at time point)/(average construct mass on day 0). One half was digested with proteinase K (MP Biomedical, Santa Ana, CA) and the other half was digested with guanidine. Samples were lyophilized prior to the proteinase K digestion (0.5 mg/ml) as previously described (Hollander et al., 1994). Guanidine digestion was performed with 4 M guanidine HCl at 4 °C for 16 hours. GAG, collagen, and pyridinoline content were measured from the proteinase K digests. GAG content was assayed using the 1,9 dimethylmethylene blue dye-binding (DMMB) assay

(Farndale et al., 1986). Collagen and pyridinoline content were assayed after acid hydrolysis of the digests using an ortho-hydroxyproline (OHP) assay (Stegemann and Stalder, 1967) and a pyridinoline specific enzyme linked immunosorbent assay (ELISA; Quidel Corperation, San Diego, CA), respectively. Pyridinoline content was not measured on day 0 due to the low collagen content (~ 0). A 1:7.64 OHP:total collagen mass ratio was used to determine collagen content (Hollander et al., 1994). COMP was measured from the guanidine digests with a COMP specific ELISA (MDBiosciences, St. Paul, MN). GAG and COMP were measured in the conditioned media samples directly, without digestion, using the DMMB assay and COMP ELISA, respectively. Media samples were pooled between two media changes for the COMP assay and the mass of COMP released into the media was averaged over the span of the two sequential media changes. Collagen media concentrations were assayed via the OHP assay of acid-hydrolyzed media samples. Pyridinoline content is presented both as a concentration and a molar fraction to collagen: mol pyridinoline/mol collagen triple helix (collagen triple helix MW = 285 kDa) (Grant and Prockop, 1972).

Statistics

The biochemical concentrations, equilibrium compressive modulus E_Y, hydraulic permeability k, equilibrium tensile modulus E_T, and normalized disk volume (disk volume normalized to day 0 volume) of the constructs were compared with a two-way analysis of variance (ANOVA) using Tukey's HSD post-hoc test ($\alpha = 0.05$). Synthesis rates were compared with an analysis of covariance of the cumulative mass per construct released to the media and the mass accumulated in the scaffold over the culture time (day 0 to 45 for the control and β3+ groups and day 14 to 45 for the β3– group) (Sokal and Rohlf, 1995). Retention fractions for each matrix constituent were compared using an ANOVA of each group's mean, uncertainty, and n (total number of constructs and media aliquots for each supplementation group) (Cohen, 2002). Data are reported as mean ± standard deviation (for GAG, collagen, mechanical properties, and swelling ratio, $n = 4$; for COMP and pyridinoline, $n = 3$). For each group and constituent, the fit between the experimental and binding kinetics model was determined by nonlinear regression for

both the construct matrix (sum of bound and soluble matrix within the construct) and cumulative matrix media release.

Human Patella-Sized Construct Model

Computational Anatomical Model

Three-dimensional finite element model of the patella construct was constructed from the anatomical human patella surfaces obtained using stereophotogrammetry (Ateshian et al., 1992; Ateshian et al., 1991; Hung et al., 2003). The cellular agarose gel construct was modeled atop a porous bone scaffold. To model the experimental conditions, in which the porous trabecular bone scaffold was filled with the chondrocyte-embedded agarose gel, the scaffold was also modeled with a cellular component (Figure S2A). The gel construct was seeded at 60×10^6 cells/mL; this cell density informs both the matrix synthesis and nutrient consumption rates. Likewise, the consumption and synthesis parameters in the bone scaffold region were based on trabecular bone having a porosity of 80% (trabecular bone porosity > 70%; (Schaffler and Burr, 1988)); therefore the effective cell density within the scaffold was 48×10^6 cells/mL. The model was analyzed with the FEBio finite element software (www.febio.org) which incorporates transport mechanics and chemical kinetics. We have included a table outlining the salient features of this model and the synthesis model presented in the manuscript here (Table S1).

Culture Conditions

In the model, the construct was surrounded with a bath containing 75 mL of media (Supp. Figure 2B). The media and construct glucose concentration was initially set at 25 mM and the soluble and bound matrix concentrations were initially 0 (day 0). During the culture simulation the 'cells' within the construct and scaffold consumed glucose and synthesized soluble matrix, thereby decreasing glucose concentration and increasing soluble ECM product concentration in the construct and surrounding media. Glucose was consumed according to the consumption rate measured experimentally as described below; matrix was synthesized according to the rates measured as described in the main text. As the original

patella construct experiment was performed in the absence of TGF-β3 supplementation, the synthesis and binding parameters found for the 'control' case (Table 1) were used in the model simulation. Consistent with the experiment, the media in the model was 'changed' three times per week (in a 2-2-3 day sequence) over the 35-day culture. Media changes consisted of resetting the media solution to 25 mM glucose concentration and 0 mM soluble ECM product concentration.

Matrix Synthesis and Glucose Consumption

Three chemical reactions were modeled in this finite element analysis. Both glucose consumption and GAG synthesis were modeled according to Michaelis-Menten kinetics according to the available glucose concentration:

$$\hat{c}^{\alpha} = \frac{R^{\alpha} \times c^{Glu}}{K_m + c^{Glu}} \tag{S1}$$

where R^{α} is either the glucose consumption rate ($R^{Glu} < 0$; [nmol μL^{-1} s^{-1}]) or the GAG synthesis rate ($R^{GAG} > 0$; [nmol μL^{-1} s^{-1}]). Therefore, the three equations modeled were: (1) Glucose uptake by cells according to equation (S1) where $\hat{c}^{\alpha} = \hat{c}^{Glu}$; here the maximal cellular glucose consumption rate, R^{Glu}, was experimentally determined (below) and the Michaelis constant, K_m = 0.35 mM, was taken from previous experiments on chondrocytes (Windhaber et al., 2003). (2) Soluble GAG synthesis was modeled according to equation (S1) where $\hat{c}^{\alpha} = \hat{c}^{GAG}$ and the maximal synthesis rate, R^{GAG}, was taken from the previous experimental synthesis results (scaled appropriately for the cellularity of both the gel construct and scaffold) and the Michaelis constant, K_m, was the same as the glucose consumption reaction. Additionally, based on our earlier finding that low levels of glucose results in no significant ECM deposition (Cigan et al., 2013), a nutrient threshold level was added to the synthesis equation, such that ECM synthesis was completely inhibited within regions where the glucose concentration was below the threshold level. (3) GAG deposition was modeled using standard reversible binding kinetics of the soluble GAG with the extracellular matrix, based on the parameters curve-fitted to the experimental data of this study.

The following additional experiments were performed to identify the remaining necessary parameters (cellular glucose consumption rate and ECM nutrient threshold) for this system:

Glucose Consumption Rate

Constructs (∅4 mm × 2.34 mm thick, 10 × 10^6 cells/mL in 2% agarose gel) were cultured as previously described for 7 weeks. On weeks 1, 3, 5, and 7, media samples were taken 4, 8, 24, 48 and 72 hours after a media change (n = 3 for each time) and assayed for glucose (Amplex Red Glucose Assay, Invitrogen) and DNA content. The glucose consumption rate was calculated from the slope of the glucose media loss over 72 h (Figure S2). The average glucose consumption rate was calculated to be 1.24 ± 0.35 × 10^{-13} mol $cell^{-1}$ hr^{-1} during the seven week culture. This level of glucose consumption was similar to previously measured consumption rates of bovine chondrocytes both in monolayer and three-dimensional culture (Marcus, 1973; Obradovic et al., 1999).

ECM Nutrient Threshold

Based on our prior work identifying glucose as a critical nutrient for this CTE system, it was necessary to find the critical concentration of glucose needed to sustain normal ECM deposition. Constructs (∅4 mm × 2.34 mm thick, 30 × 10^6 cells/mL in 2% agarose gel) were cultured as previously described for 6 weeks. Media were prepared using glucose-free DMEM, and glucose was supplemented to produce 0.17×, 0.5×, 0.67×, 0.83×, and 1× the levels of glucose present in typical hgDMEM (4.5 mg/L = 25 mM). Constructs were taken on day 42 for mechanical (E_Y) and biochemical testing (GAG, collagen, DNA) as previously described. E_Y, GAG, collagen, and DNA were statistically similar between the 0.5×, 0.67×, 0.83× groups and the 1× group after 6 weeks (Table S2). The 0.17× supplementation group, however, failed to accumulate significant GAG and collagen, experiencing decreased cellularity, and exhibiting significantly poorer mechanical properties. There was also a decrease in the construct cellularity in the 0.17× group, which could also decrease the ECM synthesis capacity of GAG and collagen in addition to the low nutrient availability of the treatment. Accordingly, for modeling the patella, we chose a level of 0.5× (12.5 mM) as the critical glucose concentration necessary for ECM synthesis.

Correlations between Mechanical Properties and Biochemical Composition

E_Y showed a high correlation with GAG concentration (Figure S4A; $R^2 = 0.74$). Relatively low correlations were found for E_Y versus collagen or COMP (Figure S4B; $R^2 = 0.31$ and Figure S4C; $R^2 = 0.32$, respectively). E_Y was moderately correlated to pyridinoline concentration (Figure S4D; $R^2 = 0.47$). The swelling ratio displayed a high correlation to GAG concentration (Figure S4E; $R^2 = 0.74$), a moderate correlation to collagen concentration (Figure S4F; $R^2 = 0.48$), a poor correlation to COMP (Supp. Fig. 4G; $R^2 = 0.27$), and a moderate correlation to pyridinoline (Figure S4H; $R^2 = 0.56$). E_T was moderately correlated with GAG and pyridinoline (Figure S4I; $R^2 = 0.49$ and Figure S4L; $R^2 = 0.50$, respectively) and poorly correlated with collagen and COMP (Figure S4J; $R^2 = 0.20$ and Figure S4K; $R^2 = 0.33$, respectively).

Figure Captions

Figure S1: (A) Schematic for the experimental set-up idealized in the matrix-binding-diffusion model. (B) A representative result of the bound matrix spatial distributions within the tissue phase of the construct (GAG accumulation in the β3− group).

Figure S2: (A) Finite element mesh and geometric model of the anatomical patella construct supported on the porous, chondral scaffold which is embedded with a cellular agarose gel, and (B) a cross sectional image of the construct surrounded within the 75 mL bath.

Figure S3: The average depletion of media glucose due to chondrocyte consumption over a 72 hour period (data represents the mean and standard deviations of the values from weeks 1, 3, 5, and 7 of culture).

Figure S4: Correlations between the mechanical properties E_Y (A-D), swelling ratio (E-H) and E_T (I-L) and the biochemical concentrations of GAG (A, E, I), collagen (B, F, J), COMP (C, G, K) and pyridinoline (D, H, L).

169

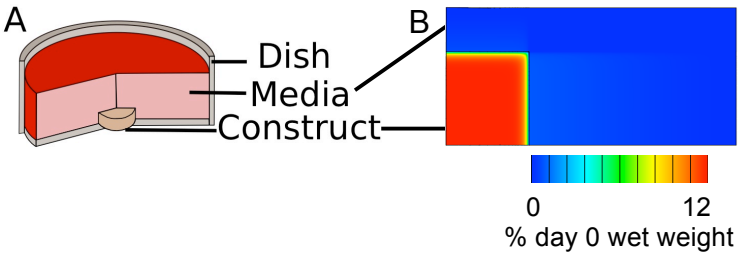

Figure S1

170

171

171

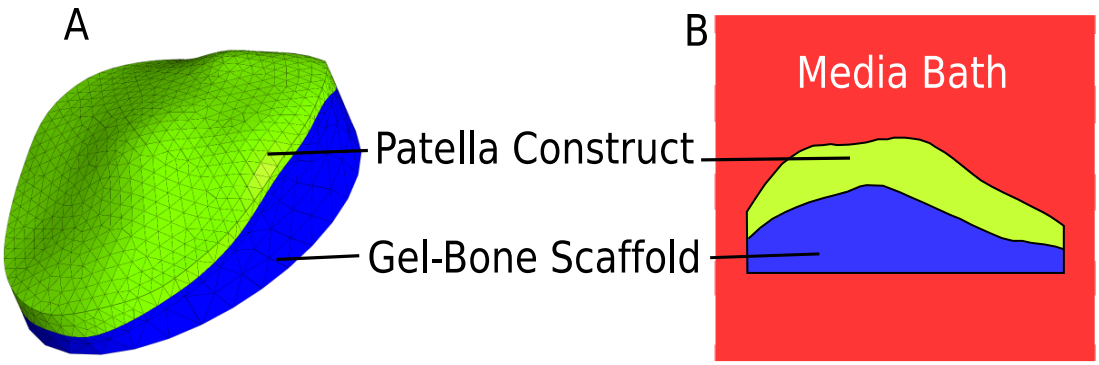

Figure S2

172

172

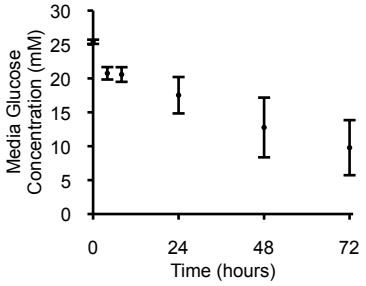

Figure S3

173

173

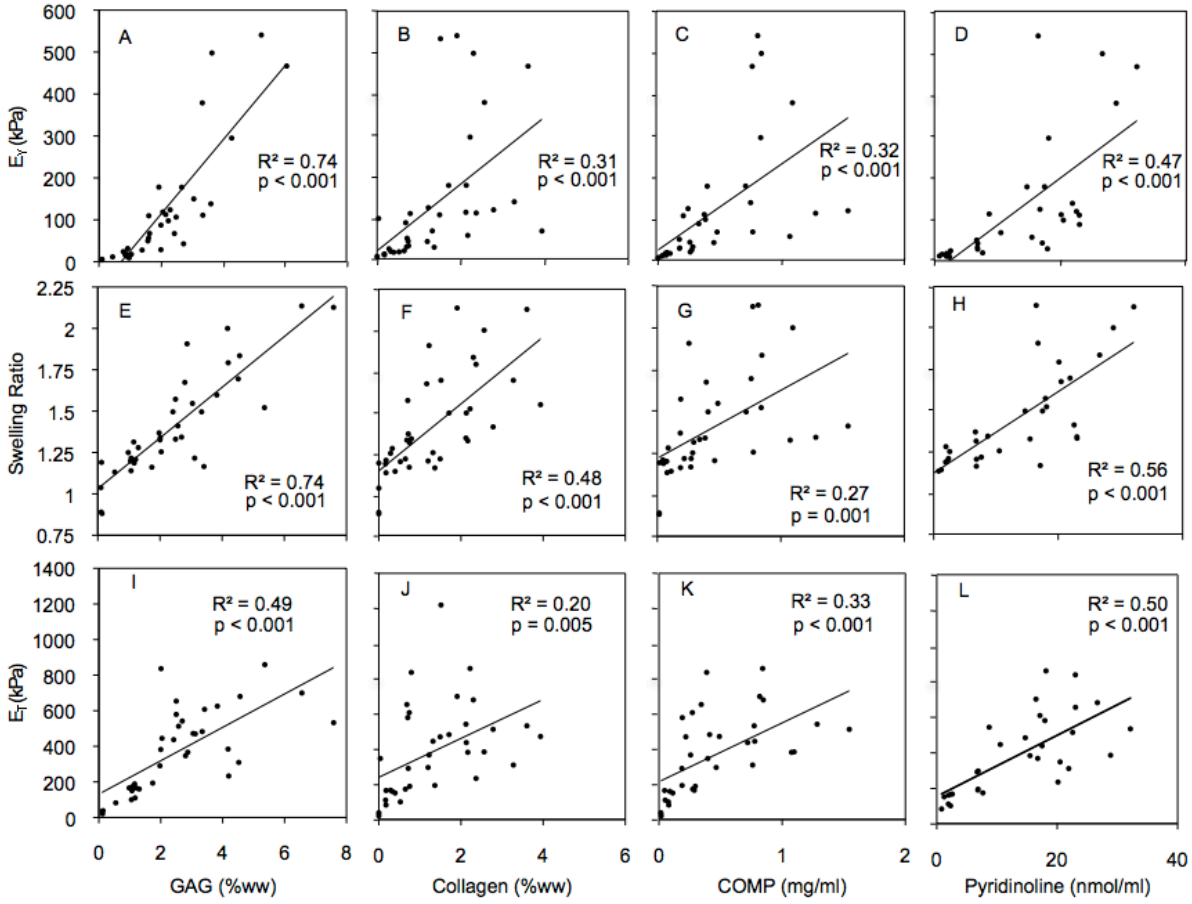

Figure S4

174

Table S1

A. Small construct synthesis model		
$\hat{c}_{syn}^{\alpha}$	Matrix synthesis rate	[nmol μL^{-1} s^{-1}]
$k_f{}^{\alpha}$	Matrix forward-binding rate	[mM^{-1} s^{-1}]
$k_r{}^{\alpha}$	Matrix reverse-binding rate	[s^{-1}]
N_t	Matrix binding-site density	[mM]
D_o^{α}	Matrix diffusivity in free solution	[mm^2 s^{-1}]
D^{α}	Matrix diffusivity in construct	[mm^2 s^{-1}]
φ_s	Solid volume fraction of construct	[-]
B. Large patella-construct model		
R^{GAG}	GAG synthesis rate	[nmol μL^{-1} s^{-1}]
$k_f{}^{GAG}$	GAG forward-binding rate	[mM^{-1} s^{-1}]
$k_r{}^{GAG}$	GAG reverse-binding rate	[s^{-1}]
N_t	GAG binding-site density	[mM]
K_m	Michaelis constant	[mM]
R^{Glu}	Glucose consumption rate	[nmol μL^{-1} s^{-1}]
c_o	Glucose concentration threshold for GAG synthesis	[mM]
D_o^{α}	Glucose/GAG diffusivity in free solution	[mm^2 s^{-1}]
D^{α}	Glucose/GAG diffusivity in agarose and agarose/bone construct	[mm^2 s^{-1}]
φ_s	Solid volume fraction of agarose and agarose/bone construct	[-]

Table S1: The model parameters for (A) the matrix synthesis model used to characterize the reversible binding rates (α = GAG, collagen, COMP; s = agarose-gel scaffold) and (B) the large patella-construct featuring glucose concentration dependent GAG synthesis and reversible GAG binding (α = GAG, glucose; s = agarose-gel and agarose-filled chondral scaffold).

Table S2

		E_Y [kPa]	GAG [%ww]	Collagen [%ww]	DNA [μg/disk]
(1)	0.17×	$30 \pm 28^{2,3,4,5}$	$1.51 \pm 0.32^{2,3,4,5}$	$0.64 \pm 0.19^{3,4}$	$7.08 \pm 1.47^{2,3,4,5}$
(2)	0.5×	481 ± 100^{1}	5.93 ± 0.27^{1}	1.33 ± 0.50	11.05 ± 0.50^{1}
(3)	0.67×	365 ± 170^{1}	5.90 ± 0.56^{1}	1.77 ± 0.62^{1}	9.86 ± 0.48^{1}
(4)	0.83×	482 ± 145^{1}	4.76 ± 1.66^{1}	1.74 ± 0.67^{1}	10.95 ± 0.54^{1}
(5)	1×	449 ± 158^{1}	4.76 ± 0.65^{1}	1.28 ± 0.33	11.50 ± 1.21^{1}

Table S2: Mechanical (E_Y) and biochemical (GAG, collagen, and DNA content) results after 6 week culture of constructs supplemented at each media change with either 0.17×, 0.5×, 0.67×, 0.83×, or 1× glucose levels (1× corresponds to typical 25 mM supplementation). The superscripts within each outcome indicate the treatments between which there is a significant difference ($p < 0.05$).

Reference:

Ateshian, G.A., Rajan, V., Chahine, N.O., Canal, C.E., Hung, C.T., 2009. Modeling the matrix of articular cartilage using a continuous fiber angular distribution predicts many observed phenomena. Journal of Biomechanical Engineering 131, 061003.

Ateshian, G.A., Rosenwasser, M.P., Mow, V.C., 1992. Curvature characteristics and congruence of the thumb carpometacarpal joint: differences between female and male joints. Journal of Biomechanics 25, 591-607.

Ateshian, G.A., Soslowsky, L.J., Mow, V.C., 1991. Quantitation of articular surface topography and cartilage thickness in knee joints using stereophotogrammetry. Journal of Biomechanics 24, 761-776.

Cigan, A.D., Nims, R.J., Albro, M.B., Esau, J.D., Dreyer, M.P., Vunjak-Novakovic, G., Hung, C.T.P.D., Ateshian, G.A., 2013. Insulin, Ascorbate and Glucose Have a Much Greater Influence than Transferrin and Selenous Acid on the in vitro Growth of Engineered Cartilage in Chondrogenic Media. Tissue Engineering. Part A.

Cohen, B.H., 2002. Calculating a Factorial ANOVA From Means and Standard Deviations. Understanding statistics 1, 191-203.

Farndale, R.W., Buttle, D.J., Barrett, A.J., 1986. Improved quantitation and discrimination of sulphated glycosaminoglycans by use of dimethylmethylene blue. Biochim Biophys Acta 883, 173-177.

Grant, M.E., Prockop, D.J., 1972. The biosynthesis of collagen. 1. N Engl J Med 286, 194-199.

Hollander, A.P., Heathfield, T.F., Webber, C., Iwata, Y., Bourne, R., Rorabeck, C., Poole, A.R., 1994. Increased damage to type II collagen in osteoarthritic articular cartilage detected by a new immunoassay. J Clin Invest 93, 1722-1732.

Huang, A.H., Baker, B.M., Ateshian, G.A., Mauck, R.L., 2012. Sliding contact loading enhances the tensile properties of mesenchymal stem cell-seeded hydrogels. European Cells and Materials 24, 29-45.

Hung, C.T., Lima, E.G., Mauck, R.L., Takai, E., LeRoux, M.A., Lu, H.H., Stark, R.G., Guo, X.E., Ateshian, G.A., 2003. Anatomically shaped osteochondral constructs for articular cartilage repair. J Biomech 36, 1853-1864.

Lima, E.G., Bian, L., Ng, K.W., Mauck, R.L., Byers, B.A., Tuan, R.S., Ateshian, G.A., Hung, C.T., 2007. The beneficial effect of delayed compressive loading on tissue-engineered cartilage constructs cultured with TGF-beta3. Osteoarthritis Cartilage 15, 1025-1033.

Marcus, R.E., 1973. Effect of Low Oxygen Concentration on Growth, Glycolysis, and Sulfate Incorporation by Articular Chondrocytes in Monolayer Culture. Arthritis Rheum. 16, 646-656.

Obradovic, B., Carrier, R.L., Vunjak-Novakovic, G., Freed, L.E., 1999. Gas exchange is essential for bioreactor cultivation of tissue engineered cartilage. Biotechnology and Bioengineering 63, 197-205.

Schaffler, M.B., Burr, D.B., 1988. Stiffness of compact bone: effects of porosity and density. J Biomech 21, 13-16.

Sokal, R.R., Rohlf, F.J., 1995. Biometry : the principles and practice of statistics in biological research, 3rd ed. W.H. Freeman, New York.

Stegemann, H., Stalder, K., 1967. Determination of hydroxyproline. Clin Chim Acta 18, 267-273.

Windhaber, R.A.J., Wilkins, R.J., Meredith, D., 2003. Functional characterisation of glucose transport in bovine articular chondrocytes. Pflugers Archiv-European Journal of Physiology 446, 572-577.